Low-dimensional sublattice melting by pressure: Superionic conduction in the phase interfaces of the fluorite-to-cotunnite transition of CaF_2

Salah Eddine Boulfelfel, Dirk Zahn, Oliver Hochrein, Yuri Grin, and Stefano Leoni*
Max-Planck-Institute for Chemical Physics of Solids, Nöthnitzer Str. 40, D-01187 Dresden, Germany
(Received 19 May 2006; published 28 September 2006; corrected 29 September 2006)

The pressure-induced phase transformation of calcium fluoride (CaF_2) from the cubic-fluorite-type structure ($Fm\bar{3}m$) to the orthorhombic cotunnite ($PbCl_2$) type structure (*Pnma*) is investigated from transition path sampling molecular dynamics simulations. Starting from an artificially prepared transformation route connecting fluorite to cotunnite, subsequent trajectory rectification evolved to a distinct picture of the favored mechanism. The latter is characterized by nucleation and growth of the new phase. The overall transformation mechanism was identified as a symmetry-lowering step from the cubic to the orthorhombic atomic configuration which is caused by the reorganization of one half of the octahedral voids. At the interface between the cubic and the orthorhombic structure, a pressure-induced local melting of the fluoride sublattice is observed. This produces defects that allow for the reorganization of the calcium sublattice which eventually leads to the recrystallization of the fluoride ions fixating one of the stable structures. Variation of the thermodynamic parameters shows that the mechanism is conserved over the experimentally relevant range, however with an increasing tendency towards incomplete transformation on lowering the temperature, in accordance with experiments.

DOI: 10.1103/PhysRevB.74.094106 PACS number(s): 64.70.Kb, 02.70.Ns, 07.05.Tp, 61.50.Ks

INTRODUCTION

Transformation processes between liquid and solid phases are phenomena of central importance in nature. The most fundamental transition of this kind is represented by crystallization from the melt. While this is one of the main synthetic pathways in solid state synthesis, a more peculiar phenomenon is reflected by superionic conductors, a fascinating blend of solid and liquid states that arises when only parts of a compound become liquid. In CaF_2, the fluoride sublattice is well known to melt on raising temperature. The present work is aimed at demonstrating pressure as an important thermodynamic variable governing sublattice melting in CaF_2. Recently, the tremendous technological potential of ion conducting materials based on distinct transport effects in interface regions has been reviewed.[1] Inspired by these studies we decided to explore the possible similarities between ion conduction in the interface region of CaF_2-BaF_2-CaF_2 sandwich structures[1] and phase fronts forming during pressure-induced structural transformations.

The polymorphism of CaF_2 encompasses two fundamental structural types, the (low pressure) face-centered cubic fluorite structure (space group $Fm\bar{3}m$), for which CaF_2 is the prototype compound, and the (high pressure) $PbCl_2$ type for the orthorhombic polymorph cotunnite (space group *Pnma*).[2,3] For salt-like compounds of composition AB_2, these structures offer an attractive combination of a close-packed array of A atoms and interstitial sites of different coordination number available for atom B. In the fluorite structure the Ca ions are in a cubic close-packed (*ccp*) arrangement, the fluoride ions occupy all the tetrahedral interstitial sites. In the cotunnite structure, the array of A atoms is hexagonal close-packed (*hcp*),[4] half of the fluoride ions exhibit tetrahedral coordination, the other half is placed off-center in the (ideally) octahedral voids of *hcp*, with fivefold coordination. Ca is eightfold coordinated in the fluorite structure, while the coordination number increases to nine in the denser cotunnite structure. The fluorite and cotunnite structures are also realized by the fluorides of the heavier alkaline-earth metals (Sr, Ba). The series of high-pressure structures for AB_2 composition is enriched by a plethora of other phases like EuI_2, α-PbO_2, on varying the halogen moiety, like in $CaCl_2$, or in oxide compounds like ZrO_2. Despite the chemical diversity of these compounds, the analogies in their high-pressure behavior, particularly the reappearance of the same atomic pattern among high-pressure polymorphs, hints at common features.

Experimental investigations of the mechanistic details of pressure-induced reconstructive phase transitions are complicated by the first-order thermodynamics that often causes the destruction of the crystal. Furthermore, these processes display a large pressure hysteresis. For CaF_2, the fluorite-to-cotunnite phase transition occurs in the range 9.5–20 GPa,[5] with the cotunnite phase retransforming to the fluorite phase on releasing pressure. The high-pressure polymorph can be quenched from higher temperature, 300 °C, nonetheless the crystallinity of the obtained material is poor.[3]

To shed light on the mechanism of the reconstructive phase transition we have performed isothermic-isobaric molecular dynamics simulations within a recently implemented transition path sampling scheme.[6] The latter allows investigating the transformation at the phase coexistence conditions, and is particularly suited for observing phase nucleation and growth in solid state reconstructive phase transitions. The performance of our approach has been extensively demonstrated for alkaline halogenides.[7–10]

SIMULATION DETAILS

The simulation scheme as it is described in Ref. 6 requires modeling of a first transition trajectory which is subsequently

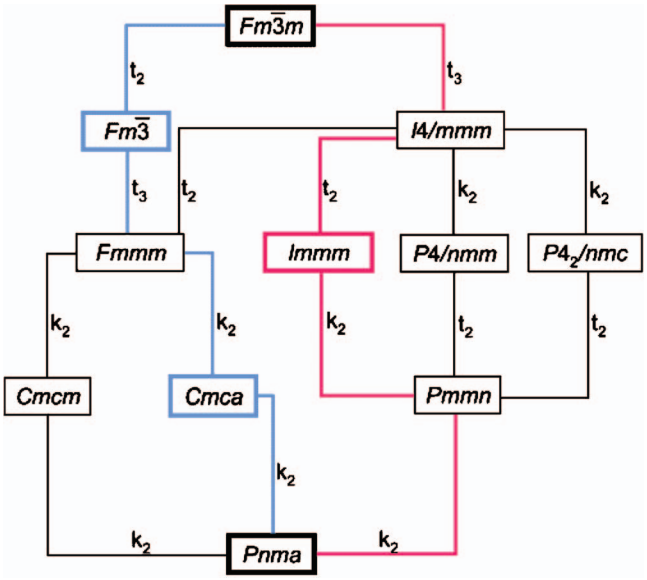

FIG. 1. (Color) Group-subgroup relation between the space group of fluorite ($Fm\bar{3}m$) and the space group of cotunnite (*Pnma*). The path used for the geometric modeling is highlighted in red, the preferred mechanism is highlighted in blue. The intermediate space groups *Immm* and *Cmca* of the first branch and the final branch are highlighted.

rectified in the course of transition path sampling iterations. Such an initial pathway can be prepared from a geometric-topological approach.[7] For this, we take advantage of the fact that the space group of fluorite is connected to the space group of cotunnite via several group-subgroups pathways.[11] The distance between the groups allows for several pathways. We have chosen the path from $Fm\bar{3}m$ to *Pnma* over *Immm* (Fig. 1, red path) as a model for the first trajectory. The transformation matrix $[(1\ \frac{1}{2}\ 0)\ (-1\ \frac{1}{2}\ 0)\ (0\ 0\ 1)]$ $[\frac{1}{4}\ 0\ \frac{1}{4}]$ was applied on the unit cell of the fluorite structure. In a common cell the atomic coordinates were varied between two limiting parameter regions corresponding to the CaF_2 and $PbCl_2$ structural motifs. From these interpolated configurations a dynamical intermediate was derived, and from it a first transition pathway, by propagating in both directions of time.[6,7] The mechanism we used for preparing the first transition trajectory contained a symmetric intermediate configuration, as it is shown in Fig. 2(b). This intermediate features trigonal prisms of Ca^{2+} ions that are formed by the fusion of adjacent tetrahedral on increasing the puckering of the layers of the cubic structure.

While this initial trajectory does not need to be a likely one, more probable routes are more frequently produced, and the trajectory regime quickly departs from the disfavored, symmetric intermediate structure, and shifts towards a preferred mechanistic regime characterized by nucleation and growth. This pathway evolution occurred within 15–20 iterations. From the first dynamical pathway, obtained from the starting model, new trajectories are iteratively produced.[6] A configuration is selected from a previous trajectory, and modified for the next simulation step keeping the total momentum, total energy, and angular momentum unchanged.

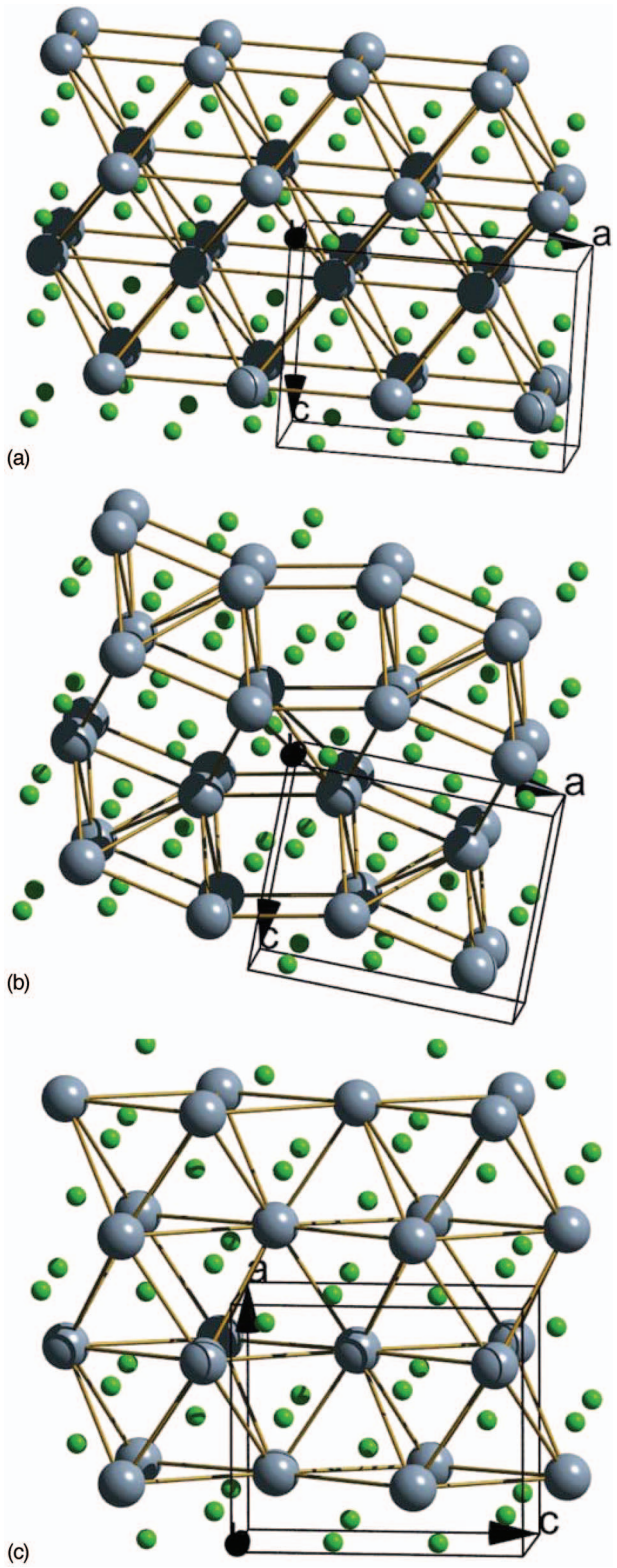

FIG. 2. (Color) Geometric model used as a starting transformation route (F green, Ca grey). The symmetry reduction from the cubic to the orthorhombic structure corresponds to a path from $Fm\bar{3}m$ to *Pnma* over *Immm* (cf. Fig. 1). a) Cubic structure, b) intermediate, space group *Immm*, c) orthorhombic structure. The cubic and orthorhombic structures are represented in a common cell with orthorhombic metric.

TABLE I. Interatomic pair potential parameters for CaF_2.

	A (eV)	ρ (Å)	C (eV Å^6)	q^2/e^2
Ca-Ca	5.8107319	0.119628	0.0	+4
Ca-F	2954.8346	0.264043	0.14469	−2
F-F	37.930398	0.145092	0.0	+1

Upon propagation of the new configuration in both forward and backward time directions, the resulting trajectory is investigated for the fluorite-to-cotunnite transition. As a discriminating order parameter between the fluorite and cotunnite structures, the average coordination number (CN) of the fluoride ions by Ca^{2+} ions is used. It amounts to 4 for the fluorite structure, and changes to 4.5 in the cotunnite structure in continuity (half of the fluorite ions in tetrahedral coordination, CN=4, the other half in pyramidal coordination, CN=5). Intermediate structures show a CN in between. The simulation box contained 256 Ca^{2+} ions and twice as many fluoride ions. A set of empirical force field parameters were used. For the molecular dynamics simulation a time step as small as 0.1 fs was chosen, in order to ensure time reversibility. The equations of motion were integrated with the DLPOLY package.[12] Therein, the Melchionna–Nose-Hoover algorithm was used to apply constant temperature and pressure.[13] The initial simulation pressure was initially chosen as 9.5 GPa,[2] which represents the lower boundary of the hysteresis obtained from experiments, where the high-pressure structure starts forming. Experiments are performed in a temperature range of 300 to 573 K. We performed different sets of simulations at different temperatures (300, 350, 400, 450, 500, 573 K) and also varied the pressure (9.5–12 GPa). Anisotropic shape changes of the simulation box were allowed for not biasing the mechanistic analysis with respect to the experiments.

INTERATOMIC PAIR POTENTIAL

Empirical interaction potentials have been shown to perform very well in many molecular dynamics simulations of salt-like compounds. For their use in phase transitions it is crucial that the model appropriately reproduces all relevant phases. Given the too focused scope of the published force fields, that were able to cover only some of the features required by our simulation, a new empirical force field for CaF_2 was developed. Therein the ionic interactions were described by a combination of Coulomb and London potentials, and short range repulsive terms. The parameters of the Buckingham pair potential model were fitted to reproduce the equations of state of both the normal and the high-pressure modifications. A relaxed fitting procedure as implemented in the program GULP[14] was used. The input was constructed from a set of *ab initio* total energy values for configurations of the normal and high-pressure structures at different volumes. The total energy calculations were performed with the FPLO package.[15–17] The fitting error was defined as the residual of the total energies. The pair potential parameters are shown in Table I.

The equilibrium lattice parameter of the cubic modification calculated with our pair potential (at 0 K), $a=536.9$, is only 1.7% smaller than the experimental value of 546.2 pm (Ref. 18) obtained by x-ray scattering. The calculated[14] bulk modulus of the normal pressure modification of CaF_2 is 97.9 GPa (at 0 K) which is 8.5% larger than the experimental value of 90.2 GPa (extrapolated to 0 K, from Ref. 19). The elastic constants, $C_{11}=166.2$, $C_{12}=63.8$, $C_{44}=55.34$ GPa, agree reasonably with experimental values ($C_{11}=165.4$, $C_{12}=44.4$, $C_{44}=34.2$ GPa).[20] Moreover, the developed pair potential is able to reproduce the temperature-induced transition from fluorite-type CaF_2 to a superionic phase on raising temperature, as well as the melting transition.[21]

The axial ratios a/b and c/b are good indicators for the adequate description of the structure under pressure as they strictly reflect the close-packed arrangement of Ca^{2+} ions. The calculated ratios are $a/b=1.665$ and $c/b=1.943$, in excellent agreement with the experimental values.[2]

RESULTS AND DISCUSSION

The way of reconstructing the Ca close-packed hexagonal pattern coded in the starting route [Figs. 2(a)–2(c)] disappears during the early iteration steps, and a different mechanism sets in. The latter involves shearing of Ca (100) layers, like it is described in the following. The mechanistic analysis is based on more than 100 transition pathways sampled after decorrelation of the trajectories from the initial, disfavored regime.

The signature of the onset of the cubic-to-orthorhombic phase transition is an enhanced mobility of the fluoride ions [Figs. 3(a)–3(d)]. While the arrangement of the Ca^{2+} ions remains as in the fluorite structure, the F^- ions can switch between different tetrahedral voids, with excursions as long as 650 pm. In the fluorite structure all tetrahedral voids are occupied. Anion mobility is achieved through the creation of a Frenkel defect, by episodic occupation of an octahedral void [Figs. 3(a) and 3(b)], leaving an empty tetrahedral void behind. The face-sharing arrangement of occupied tetrahedral and octahedral voids represents a less favored configuration, as it implies local F-F contacts that are shorter ($d \leqslant 0.433a$, a=lattice parameter) than in the fluorite structure [$d=1/2a$, Fig. 3(b)]. This configuration is quickly abandoned by migration of another fluoride ion into an octahedral void, whereby an additional tetrahedral vacancy is formed [Fig. 3(e)]. In this less dense part of the structure the reconstruction of the Ca sublattice [Figs. 3(e) and 3(f)] is initiated. Displacements of portions of (100) Ca layers along [011] with respect to the fluorite structure remove the central octahedral void [Figs. 3(e) and 3(f), right]. This is accompanied by the formation of an octahedral void with a different orientation, that shares a face with an adjacent occupied octahedral void. The fluoride ions inside these octahedra move off-center in pyramidal coordination, such that short contacts are avoided. A displacement within an adjacent (100) Ca layer rearranges another octahedron [Fig. 3(g)]. This second

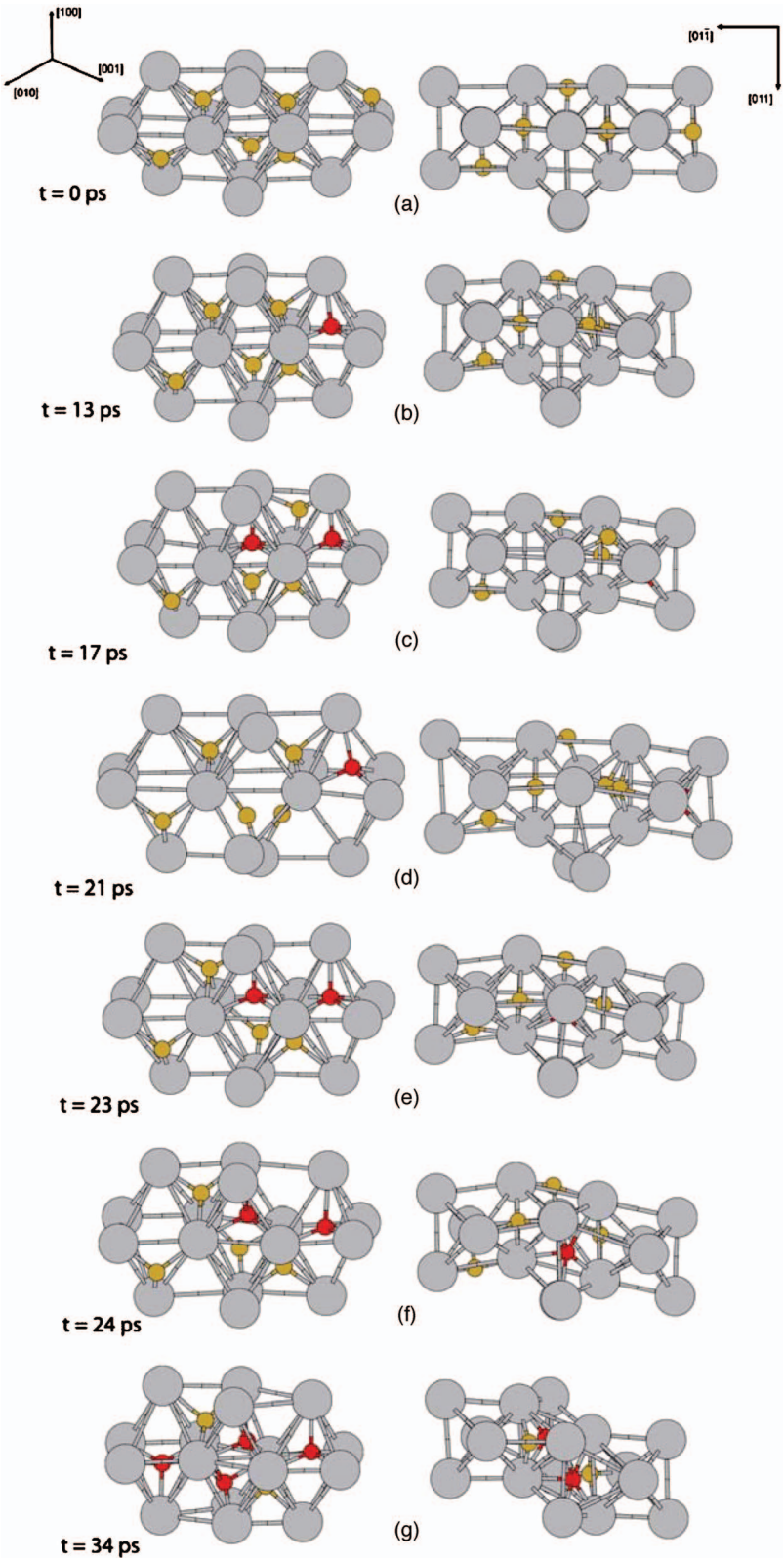

FIG. 3. (Color) Snapshots from a typical converged transition trajectory illustrating the local changes in the atomic configurations and the mechanism transforming the cubic (upper part) into the orthorhombic (lowest part) structure. Three adjacent octahedra are shown. Grey—calcium, red—fluoride ions in octahedral voids, orange—fluoride ions in tetrahedral voids.

new octahedron shares a face with an octahedron of the pristine cubic structure and an edge with the previously formed new octahedron. Again the fluoride ions occupy the one half of the octahedron (a pyramid) where no short contacts to fluoride ions are formed.

In the cubic close-packed arrangement the centers of the octahedral voids are connected by a single translation, which is reflected in the equal orientation of the octahedra [Fig. 3(a), right]. The overall reconstruction of the Ca sublattice during the phase transition rearranges half of them, which

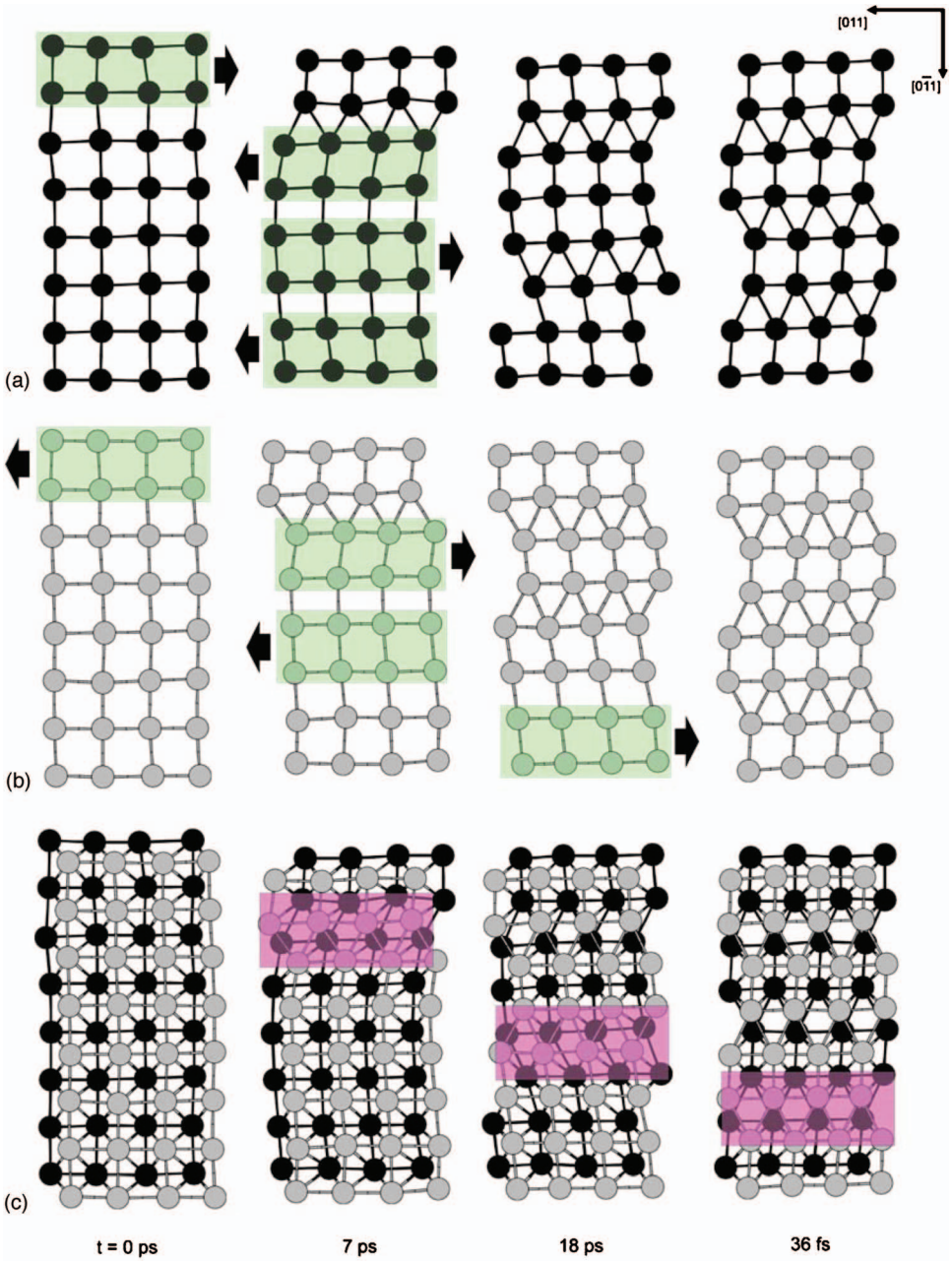

FIG. 4. (Color) Reconstruction of the Ca sublattice by layer shearing along [011] (red stripes in c). Green stripes highlight pattern of antiparallel shifts within adjacent (100) layers. The two layers are represented separately for better visibility. c) Two adjacent (100) layers a) upper layer b) lower layer.

results into two distinct sets of octahedral voids. This atomic movement is the symmetry-lowering step.

The reconstruction of the Ca sublattice is achieved by shearing of layers along [011] [Fig. 4(c), red stripes]. In adjacent (100) layers (4^4 square nets) this involves antiparallel shift of "ladders" of Ca^{2+} ions [green bands in Figs. 4(a) and 4(b)], such that new octahedral voids are formed in between, and the square nets are rearranged into 3^34^2 nets, with rows of triangles.

The simulation procedure allows assessing the probability of obtaining phase B starting from phase A.[22] The equilibrium situation, $\Delta G=0$, corresponds to an equal probability to reaching phase A from B, and vice versa. Following the formalism given in Ref. 22 we use the index $\ln(\alpha_{\text{fluorite}}/\alpha_{\text{cotunnite}})$ (α_I is proportional to the momentum modification in phase I; I=fluorite, cotunnite) as a measure of the distance from the thermodynamic equilibrium. For $p=9.5$ GPa the index is 0.87, meaning that the pressure is slightly undercritical. On enhancing the pressure ($p=12$ GPa) the system is shifted closer to phase coexistence. On lowering the temperature, the probability of getting the cubic phase is larger, and the equilibrium is shifted towards the cubic side. In this simulation regime, the tendency of forming configurations that are a patchwork of cubic and orthorhombic structure increases. This finds an echo in the increasingly poor cristallinity of the samples in quenching experiments.[3]

In the overall mechanism distinct directions for the reorganization of the Ca sublattice and for the displacement of F^- ions appear. In Fig. 5(a) an early stage of the overall reconstruction is shown. Ca^{2+} ions displace along [011], vertically in Fig. 5. The movement of fluoride ions has been traced by

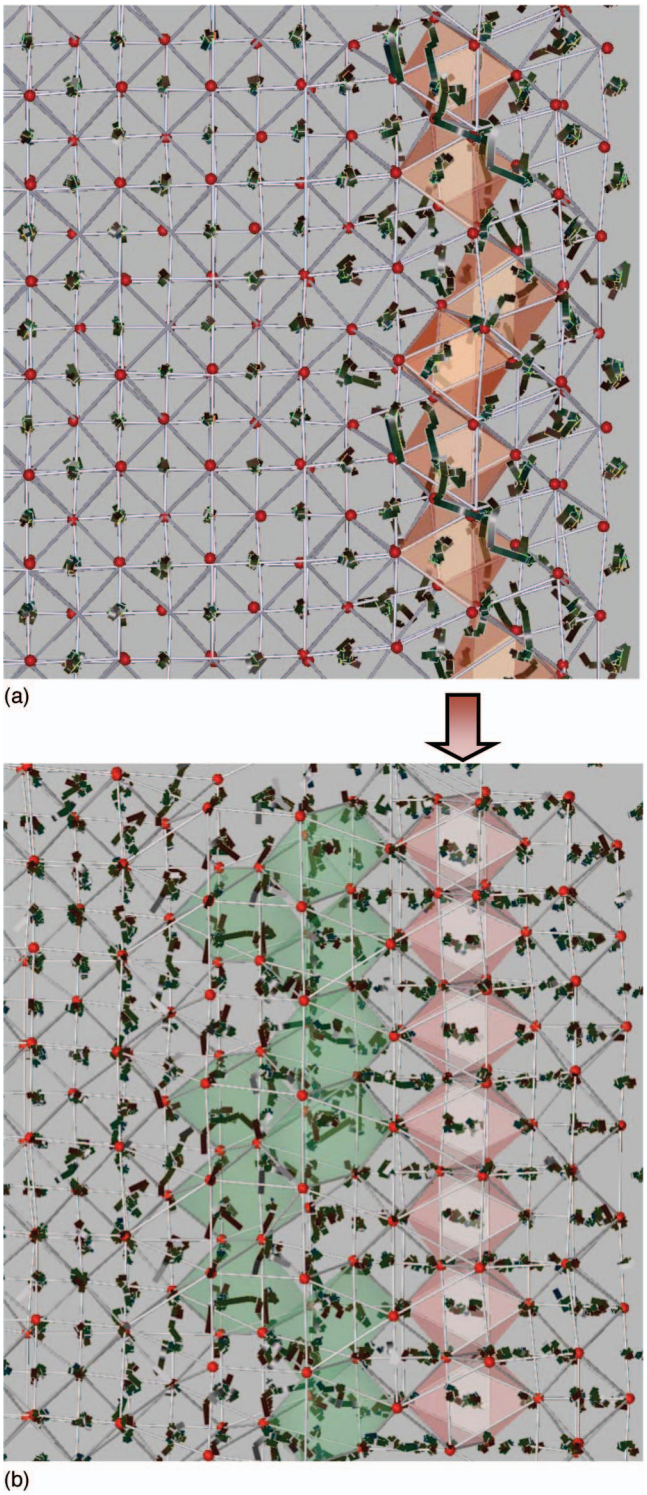

FIG. 5. (Color) Snapshots from a typical trajectory illustrating the different mobility of fluoride ions at different times and different places of the reconstructing structure. The displacements of fluoride ions are traced in a time window of 1.2 ps. The Ca^{2+} ions are shown in red. a) In the reconstructing region octahedral voids are rearranged and occupied by fluoride ions (transparent red polyhedra). Only in this region anion mobility is observed. b) Shift of the phase propagation front. Anion mobility is enhanced only in the interface region (green polyhedra) between cubic (left) and orthorhombic atomic pattern.

"illuminated lines"[23] over a period of 1.2 ps. This emphasizes the different mobility of fluoride ions in different regions and at different stages of the transforming box. F^- ions that are still in the fluorite configuration (left) display a short trace, while F^- ions in the interfacial region (right) exhibit an enhanced mobility reflected by a longer trace. Furthermore, they form chains that propagate diagonally in the box [Fig. 5(a)]. The "jumps" are frequent in the regions where octahedra are reconstructing (red polyhedra) and reach out to neighboring regions, where the reconstruction is about to start. While the overall F^- ions displacement follows crystallographic directions, the local jumps are uncorrelated, such that this region is liquid-like. The setup of an interfacial region hence corresponds to a local melting of the F sublattice. Upon propagation of the phase front [Fig. 5(b), green polyhedra], the liquid-like interface is shifted such that enhanced mobility characterizes this region only. This picture is intrinsically different from a conventional solid-solid transformation. In the latter, the displacement paths of rearranging atoms are well defined in both direction and length.

In terms of symmetry, the initial path over the *Immm* intermediate is quickly abandoned (Fig. 1, red path), and a different path is found in the course of our molecular dynamics simulation (Fig. 1, blue path). The important step highlighted in the analysis described above (Fig. 3) lies in the reorientation of half of the octahedral voids of the fluorite structure. Upon occupation of different octahedral voids by fluoride ions the latter become different in symmetry, because the (centering) vector connecting the octahedra is extinguished. At the same time, the fluoride ions are trapped in their final position, effectively condensating from the liquid-like interface into the final cotunnite structure. The path over the *Cmca* intermediate (Fig. 1, blue pathway) allows a splitting of the fluoride positions (crystallographic and dynamic at the same time) and corresponds to the preferred mechanism identified from our simulations. Considering the details of the mechanism, the *translationsgleich* (*t*) branch of the path ($Fm\bar{3}m$-$Fm\bar{3}$-*Fmmm*) corresponds to the superionic region characterizing the interface, the *klassengleich* (*k*) segment (*Fmmm-Cmca-Pnma*) hosts the reconstructive steps, and corresponds to a phase front propagation step (Fig. 5, red polyhedra) involving freezing of the anionic sublattice and formation of structural motifs of the new phase.

In summary, the transition is initiated by fluoride ions switching to octahedral voids in the close-packed Ca sublattice. The locally liquid anionic sublattice causes Frenkel defects that enable the modification of an otherwise dense and rigid close-packed atomic arrangement. This occurs by antiparallel Ca layer shearing along [011] and reorganization of half of the pristine octahedral voids. The momentarily occupation of octahedral voids causes short F-F contacts in terms of adjacent face-sharing tetrahedra. This unfavorable configuration is resolved by a local geometric change that reorients the octahedron. This induces a propagation of the phase interface causing the "freezing" of the formerly mobile fluoride ions. Further propagation of the phase front is carried by liquid-like fluoride ions that reach out to adjacent layers.

The nucleation and growth scenario accessible through our simulation resolves different symmetry lowering steps

into different regions of the simulation cell. Not only can the global mechanism be identified. The fine granularity of the simulations allow identifying the chemical aspects of symmetry lowering steps: the formation of a liquid-like interface, and therein the rules of avoiding face-sharing arrangements that "push" the fluoride ions in the right adjacent voids, leading to freezing of the fluoride sublattice.

The observation of this phenomenon is closely connected to the applied simulation scheme which allows the unbiased identification of transformation mechanisms,[6] domain formation, and interface geometries.[24] Nevertheless, interface-based ionic mobility was identified in CaF_2-BaF_2-CaF_2 sandwich structures.[1] As the identified superionic conduction state only occurs in an interfacial region of the two stable phase domains a direct experimental observation appears rather difficult. However, within the few picoseconds of liquid-like mobility of a single fluorite $\rightarrow$cotunnite$\rightarrow$fluorite cycle, the fluoride ions diffuse by more than 1 nm. Repeated transitions may hence lead to a percolation of the F sublattices of the stable states that should in principle be accessible to the experiment.

CONCLUSIONS

In conclusion, we performed transition path sampling molecular dynamics runs of the phase transition of calcium fluoride induced by pressure. Using a pathway obtained from a geometric mechanism as starting route, developed on the basis of group-subgroup relationships, the simulations converged to a favored mechanistic regime, characterized by coexisting phases separated by a two-dimensional interface. Therein the liquid-like mobility of the fluoride ions causes the formation of Frenkel defects that allow for the reconstruction of the dense Ca sublattice. Phase propagation occurs on shifting the phase front, under freezing of the locally liquid fluoride ions sublattice into the new phase, and melting in the interfacial region. The enhanced mobility of the anions in confined, low-dimensional interfacial regions recalls the temperature-induced phenomenon of superionic conduction in bulk materials. In this work we demonstrated pressure as the thermodynamic parameter behind sublattice melting.

ACKNOWLEDGMENTS

The authors wish to thank Rüdiger Kniep for fruitful discussions. S.L. acknowledges the Swiss Science Foundation for funding.

*Email address: leoni@cpfs.mpg.de

[1] J. Maier, Nat. Mater. **4**, 805 (2004).
[2] K. F. Seifert, Ber. Bunsenges. Phys. Chem. **70**, 1041 (1966).
[3] E. Morris, T. Groy, and K. Leinenweber, J. Phys. Chem. Solids **62**, 1117 (2001).
[4] B. G. Hyde, M. O'Keeffe, W. M. Lyttle, and N. E. Brese, Acta Chem. Scand. **46**, 216 (1992).
[5] L. Gerward *et al.*, J. Appl. Crystallogr. **25**, 578 (1992).
[6] D. Zahn and S. Leoni, Phys. Rev. Lett. **92**, 250201 (2004).
[7] S. Leoni and D. Zahn, Z. Kristallogr. **219**, 345 (2004).
[8] D. Zahn and S. Leoni, Z. Kristallogr. **219**, 339 (2004).
[9] D. Zahn, O. Hochrein, and S. Leoni, Phys. Rev. B **72**, 094106 (2005).
[10] D. Zahn and S. Leoni, J. Phys. Chem. B **110**, 10873 (2006).
[11] M. I. Aroyo *et al.*, Z. Kristallogr. **221**, 15 (2006).
[12] W. Smith and T. J. Forester, J. Mol. Graphics **14**, 136 (1996).
[13] Melchionna, G. Ciccotti, and B. L. Holian, Mol. Phys. **78**, 533 (1993).
[14] J. D. Gale and A. L. Rohl, Mol. Simul. **29**, 291 (2003).
[15] K. Koepernik and H. Eschrig, Phys. Rev. B **59**, 1743 (1999).
[16] H. Eschrig, *Optimized LCAO Methods and the Electronic Structure of Extended Systems* (Springer, Berlin, 1989).
[17] (a) In the scalar relativistic calculation within the LDA scheme [Ref. 17(b)] Ca($4s$,$3d$), F($2s$,$2p$,$3d$) represented the basis sets. Lower lying states were treated as core states. $3s$, $3p$ (Ca) states were included in the basis sets to avoid core-core overlaps. A k mesh of 84 (cubic structures) and 343 (orthorhombic structures) irreducible points in the Brillouin zone ensured convergence with respect to the number of k points. The spatial extension of the orbitals forming the basis was optimized to minimize the total energy. (b) J. P. Perdew and Y. Wang, Phys. Rev. B **45**, 13244 (1992).
[18] O. Hochrein *et al.* (to be published).
[19] F. Hund and K. Lieck, Z. Anorg. Allg. Chem. **271**, 17 (1952).
[20] M. Catti, R. Dovesi, A. Pavese, and V. R. Saunders, J. Phys.: Condens. Matter **3**, 4151 (1991).
[21] S. Speziale and T. S. Duffy, Phys. Chem. Miner. **29**, 465 (2002).
[22] D. Zahn, J. Solid State Chem. **177**, 3590 (2004).
[23] M. Valle, Z. Kristallogr. **220**, 585 (2005).
[24] S. Leoni and D. Zahn (to be published).